



Dissecting the Drug-receptor Interaction with the Klopman-Peradejordi-Gómez (KPG) Method-II: The Interaction of 2,5-Dimethoxyphenethylamines and their N-2-methoxybenzyl-substituted Analogs with 5-HT_{2A} Serotonin Receptors

Juan S. Gómez-Jeria*, Pablo Castro-Latorre, Camila Moreno-Rojas

Quantum Pharmacology Unit, Department of Chemistry, Faculty of Sciences, University of Chile, Las Palmeras 3425, Santiago 7800003, Chile

Abstract A study to find relationships between electronic structure and 5-HT_{2A} serotonin receptor binding affinity was carried out in a group of *para*-substituted 2,5-dimethoxyphenethylamines and their N-2-methoxybenzyl-substituted analogs. Statistically significant equations were obtained for different models of the common skeleton. An integrated affinity pharmacophore was built. The molecule-receptor interaction seems to be very complex in agreement with the high selectivity that the receptors must show to preserve the integrity of the biological system in which they are inserted.

Keywords 5-HT_{2A}, serotonin, QSAR, common skeleton, DFT, electronic structure, phenethylamines, N-2-methoxyphenethylamines, pharmacophore

Introduction

For a longtime our Unit has been interested in the analysis of the relationships between electronic structure and serotonin receptor(s) binding affinity [1-13].

In the first paper of this series we analyzed the relationships between electronic structure and 5-HT_{1A} receptor binding affinity of a group of *para*-substituted 2,5-dimethoxyphenethylamines and their N-2-methoxybenzyl-substituted analogs [14]. Here, and for the same group of molecules, we present the results of a similar study but for the relationships between electronic structure and 5-HT_{2A} receptor binding affinity. Let us remember that some of the molecules studied here belong to the 25-NB series and are extremely potent and highly selective for the 5-HT_{2A} receptor.

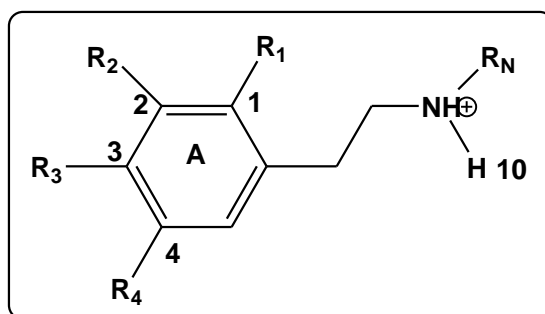


Figure 1: General formula of the molecules used in this study

Molecules and Calculations

The molecules and receptor binding results were taken from a recent publication, and are presented in Fig. 1 and Table 1. The binding affinities were measured in human 5-HT_{2A} receptor-expressing NIH-3T3 cells [15].

Table 1: 2,5-dimethoxyphenethylamines, their N-2-methoxybenzyl-substituted analogs and 5-HT_{2A} receptor binding affinity

Mol.	Name	R ₁	R ₂	R ₃	R ₄	R _N	log(K _i) 5-HT _{2A}
1	2C-B	OMe	H	Br	OMe	H	-2.07
2	2C-C	OMe	H	Cl	OMe	H	-0.89
3	2C-D	OMe	H	Me	OMe	H	-1.49
4	2C-E	OMe	H	Et	OMe	H	-1.98
5	25B-NBOMe	OMe	H	Br	OMe	2-methoxybenzyl	-3.30
6	25C-NBOMe	OMe	H	Cl	OMe	2-methoxybenzyl	-3.15
7	25D-NBOMe	OMe	H	Me	OMe	2-methoxybenzyl	-3.00
8	25E-NBOMe	OMe	H	Et	OMe	2-methoxybenzyl	-3.22
9	2C-H	OMe	H	H	OMe	H	0.20
10	2C-I	OMe	H	I	OMe	H	-2.46
11	2C-N	OMe	H	NO ₂	OMe	H	-1.63
12	2C-P	OMe	H	<i>n</i> -Pr	OMe	H	-2.09
13	25H-NBOMe	OMe	H	H	OMe	2-methoxybenzyl	-1.79
14	25I-NBOMe	OMe	H	I	OMe	2-methoxybenzyl	-3.22
15	25N-NBOMe	OMe	H	NO ₂	OMe	2-methoxybenzyl	-3.10
16	25P-NBOMe	OMe	H	<i>n</i> -Pr	OMe	2-methoxybenzyl	-2.96
17	2C-T-2	OMe	H	SEt	OMe	H	-2.05
18	2C-T-4	OMe	H	<i>S-i</i> -Pr	OMe	H	-1.55
19	2C-T-7	OMe	H	<i>S-Pr</i>	OMe	H	-2.19
20	Mescaline	H	OMe	OMe	OMe	H	0.80
21	25T2-NBOMe	OMe	H	SEt	OMe	2-methoxybenzyl	-3.22
22	25T4-NBOMe	OMe	H	<i>S-i</i> -Pr	OMe	2-methoxybenzyl	-2.80
23	25T7-NBOMe	OMe	H	<i>S-i</i> -Pr	OMe	2-methoxybenzyl	-2.96
24	Mescaline-NBOMe	H	OMe	OMe	OMe	2-methoxybenzyl	-0.85

The common skeleton

We considered four possibilities for the building of the common skeleton (see Fig. 1):

Case 1A. We hypothesized that all 24 molecules interact with the 5HT_{2A} receptor only through the aromatic ring A, the alkylamino chain and the proton. We included the orientational parameters of the substituents of ring A (Fig. 2).

Case 1B: We hypothesized that all 24 molecules interact with the 5HT_{2A} receptor only through the aromatic ring A, the alkylamino chain and the proton. We included the orientational parameters of the substituents of ring A and the orientational parameter of the 2-methoxyphenyl moiety.

Case 2. We hypothesized that all 24 molecules interact with the 5HT_{2A} receptor only through the aromatic ring A, the alkylamino chain, the proton and the first atom of the substituents attached to positions 1-4.

Case 3. We hypothesized that all 12 *N*-2-methoxybenzyl-phenethylamines interact with the 5HT_{2A} receptor only through the aromatic ring A, the alkylamino chain, the proton, the first atom of the substituents attached to positions 1-4 and the methoxybenzyl moiety (including the first atom of the methoxybenzyl substituent).

Case 4. We hypothesized that all 12 phenylalkylamines interact with the 5HT_{2A} receptor only through the aromatic ring A, the alkylamino chain, the proton and the first atom of the substituents attached to positions 1-4 (see below for each common skeleton).



This selection intends to allow the potential extraction of more information of the factors controlling the drug-receptor interaction.

To find the structure-affinity relationships we employed the Klopman-Peradejordi-Gómez (KPG) method. For details we refer the reader to the literature [16-23].

The electronic structure of all molecules was calculated within the Density Functional Theory (DFT) at the mPW1PW91/DGDZVP level with full geometry optimization [24]. The protonated forms were used. The Gaussian suite of programs was used [25]. The information needed to calculate the numerical values for the LARIs was obtained from the Gaussian results with the D-Cent-QSAR software [26]. All the electron populations smaller than or equal to 0.01 e were considered as zero [18]. Negative electron populations coming from Mulliken Population Analysis were corrected as usual [27]. Orientational parameters taken from published Tables or calculated in our Unit with the Steric software [28-30]. Since the resolution of the system of linear equations is not possible because we have not experimental data, we employed Linear Multiple Regression Analysis (LMRA) techniques to find the best solution. For each case, a matrix containing the dependent variable ($\log(\text{IC}_{50})$ in this case) and the local atomic reactivity indices of all atoms of the common skeleton as independent variables was built. Regarding the local atomic reactivity indices depending on the MO (Fukui indices and superdelocalizabilities) we have employed in this study only those associated with the frontier local molecular orbitals. The Statistica software was used for LMRA[31].

Results

Results for case 1A.

The common skeleton numbering for this case is shown below (Fig. 2).

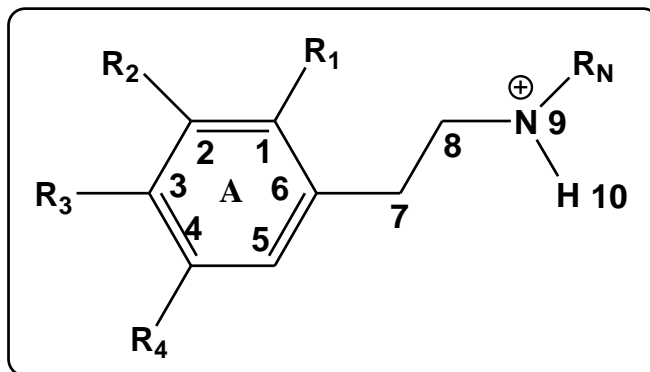


Figure 2: Common skeleton numbering for case 1A

The best statistically significant equation obtained was:

$$\log(K_i) = 0.17 - 17.55s_9 + 0.002S_9^N + 67.79F_8(\text{HOMO})^* - 2.80F_6(\text{HOMO})^* - 0.12\eta_7 \quad (1)$$

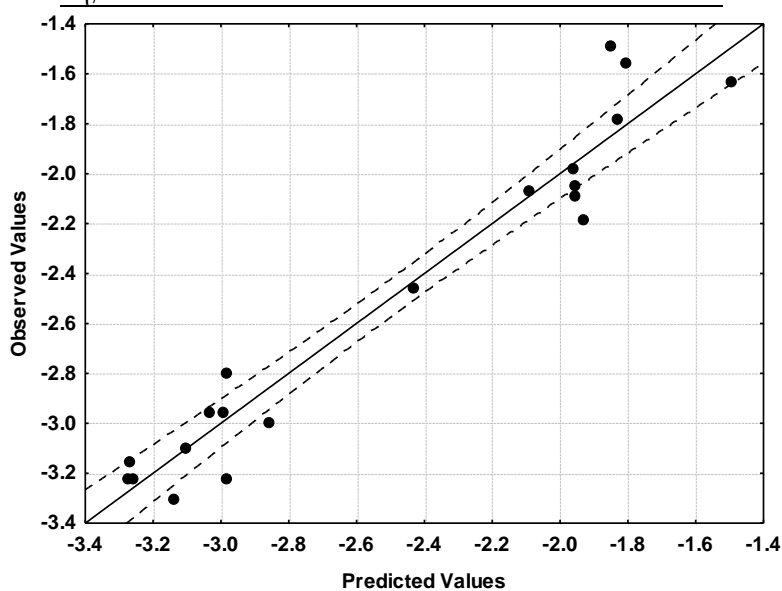
with $n=20$, $R=0.97$, $R^2=0.94$, $\text{adj-}R^2=0.92$, $F(5,14)=44.29$ ($p<0.000001$) and a standard error of estimate of 0.18. No outliers were detected and no residuals fall outside the $\pm 2\sigma$ limits. Here, s_9 is the local atomic softness of atom 9, S_9^N is the total atomic nucleophilic superdelocalizability, $F_8(\text{HOMO})^*$ is the Fukui index of the highest occupied MO localized on atom 8, $F_6(\text{HOMO})^*$ is the Fukui index of the highest occupied MO localized on atom 6 and η_7 is the local atomic hardness of atom 7. Tables 2 and 3 show the beta coefficients, the results of the t-test for significance of variable and the matrix of squared correlation coefficients for the variables of Eq. 1. There are no significant internal correlations between independent variables (Table 3). Figure 3 displays the plot of observed vs. calculated $\log(K_i)$.

Table 2: Beta coefficients and t-test for significance of coefficients in Eq. 1

Variable	Beta	t(14)	p-level
s_9	-0.84	-11.86	0.0000001
S_9^N	0.33	4.51	0.0005
$F_8(\text{HOMO})^*$	0.28	3.95	0.001
$F_6(\text{HOMO})^*$	-0.17	-2.47	0.03
η_7	-0.16	-2.25	0.04

Table 3: Matrix of squared correlation coefficients for the variables in Eq. 1

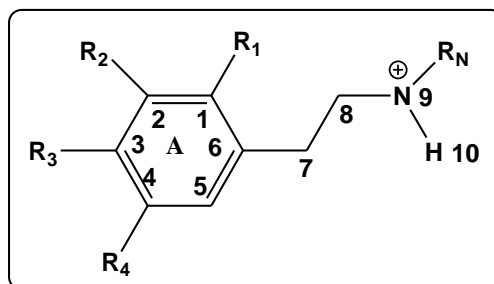
	s_9	S_9^N	$F_8(\text{HOMO})^*$	$F_6(\text{HOMO})^*$
s_9	1.00			
S_9^N	0.00	1.00		
$F_8(\text{HOMO})^*$	0.07	0.08	1.00	
$F_6(\text{HOMO})^*$	0.02	0.07	0.00	1.00
η_7	0.05	0.07	0.01	0.07

**Figure 3:** Plot of predicted vs. observed $\log(K_i)$ values (Eq. 1). Dashed lines denote the 95% confidence interval

The associated statistical parameters of Eq. 1 indicate that this equation is statistically significant and that the variation of the numerical values of a group of 5 local atomic reactivity indices of atoms of the common skeleton explains about 92% of the variation of $\log(K_i)$. Figure 3, spanning about 2 orders of magnitude, shows that there is a good correlation of observed *versus* calculated values.

Results for case 1B

The common skeleton for this case is shown below (Fig. 4).

**Figure 4:** Common skeleton numbering for case 1B

The best statistically significant equation obtained was:

$$\log(K_i) = -2.81 - 2.67F_2(LUMO)^* - 0.0005\phi_{benz} + 81.19F_8(HOMO)^* + 2.69F_3(HOMO)^* + 0.001S_9^N \quad (2)$$

with $n=20$, $R=0.98$, $R^2=0.95$, $adj-R^2=0.94$, $F(5,14)=58.53$ ($p<0.000001$) and a standard error of the estimate of 0.18. No outliers were detected and no residuals fall outside the $\pm 2\sigma$ limits. Here, $F_2(LUMO)^*$ is the Fukui index of the lowest empty MO localized on atom 2, ϕ_{benz} is the orientational parameter of the benzyl moiety, $F_8(HOMO)^*$ is the Fukui index of the highest occupied MO localized on atom 8, $F_3(HOMO)^*$ is the Fukui index of the highest occupied MO localized on atom 3 and S_9^N is the total atomic nucleophilic superdelocalizability of atom 9. Tables 4 and 5 show the beta coefficients, the results of the t-test for significance of variable and the matrix of squared correlation coefficients for the variables of Eq. 2. There are no significant internal correlations between independent variables (Table 5). Figure 5 displays the plot of observed *vs.* calculated $\log(K_i)$.

Table 4: Beta coefficients and t-test for significance of coefficients in Eq. 2

Variable	Beta	t(14)	p-level
$F_2(LUMO)^*$	-0.23	-2.71	0.02
ϕ_{benz}	-0.71	-10.39	0.0000001
$F_8(HOMO)^*$	0.33	4.97	0.0002
$F_3(HOMO)^*$	0.37	4.37	0.0006
S_9^N	0.25	4.12	0.001

Table 5: Matrix of squared correlation coefficients for the variables in Eq. 2

	$F_2(LUMO)^*$	ϕ_{benz}	$F_8(HOMO)^*$	$F_3(HOMO)^*$
ϕ_{benz}	0.00	1.00		
$F_8(HOMO)^*$	0.04	0.12	1.00	
$F_3(HOMO)^*$	0.44	0.03	0.11	1.00
S_9^N	0.02	0.00	0.08	0.00

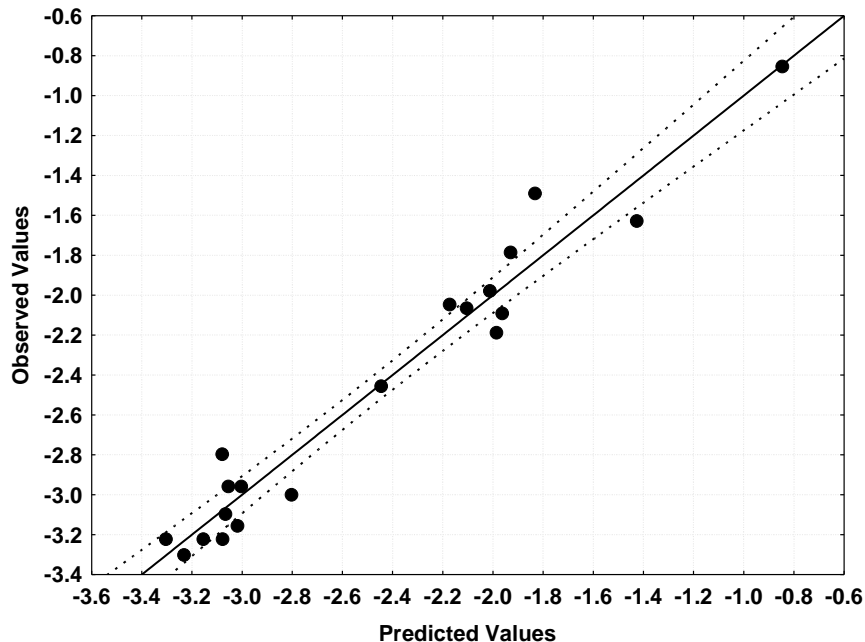


Figure 5: Plot of predicted vs. observed $\log(K_i)$ values (Eq. 2). Dashed lines denote the 95% confidence interval

The associated statistical parameters of Eq. 2 indicate that this equation is statistically significant and that the variation of the numerical values of a group of five local atomic reactivity indices of atoms of the common skeleton explains about 94% of the variation of $\log(K_i)$. Figure 5, spanning about 2.7 orders of magnitude, shows that there is a good correlation of observed *versus* calculated values and that almost all points are inside the 95% confidence interval.

Results for Case 2

The common skeleton for this case is shown below (Fig. 6).

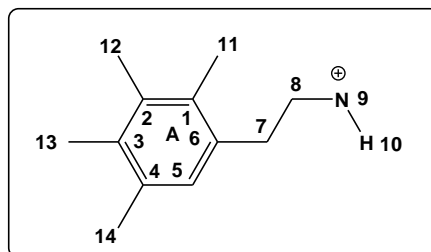


Figure 6: Common skeleton numbering for case 2

The best statistically significant equation obtained was:

$$\log(K_i) = -6.75 - 0.60\mu_9 + 0.01S_{13}^N(\text{LUMO})^* - 0.02S_1^N \quad (3)$$

with $n=19$, $R=0.97$, $R^2=0.93$, $\text{adj-}R^2=0.92$, $F(3,15)=70.65$ ($p<0.000001$) and a standard error of estimate of 0.17. No outliers were detected and no residuals fall outside the $\pm 2\sigma$ limits. Here, μ_9 is the local atomic chemical potential of atom 9, $S_{13}^N(\text{LUMO})^*$ is the orbital nucleophilic superdelocalizability of the lowest empty MO localized on atom 13 and S_1^N is the total atomic nucleophilic superdelocalizability of atom 1. Tables 6 and 7 show the beta coefficients, the results of the t-test for significance of variable and the matrix of squared correlation coefficients for the variables of Eq. 3. There are no significant internal correlations between independent variables (Table 7). Figure 7 displays the plot of observed vs. calculated $\log(K_i)$.

Table 6: Beta coefficients and t-test for significance of coefficients in Eq. 3

Variable	Beta	B	t(15)	p-level
μ_9	-0.94	-0.60	-13.72	0.0000001
$S_{13}^N(\text{LUMO})^*$	0.47	0.01	6.98	0.000004
S_1^N	-0.24	-0.02	-3.64	0.002

Table 7: Matrix of squared correlation coefficients for the variables in Eq. 3

	μ_9	$S_{13}^N(\text{LUMO})^*$	S_1^N
μ_9	1.00		
$S_{13}^N(\text{LUMO})^*$	0.00	1.00	
S_1^N	0.03	0.00	1.00

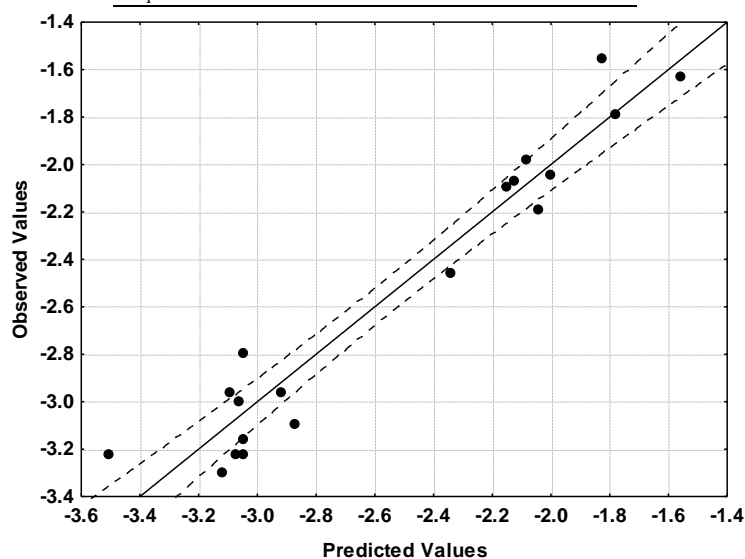


Figure 7: Plot of predicted vs. observed $\log(K_i)$ values (Eq. 3). Dashed lines denote the 95% confidence interval



The associated statistical parameters of Eq. 3 indicate that this equation is statistically significant and that the variation of the numerical values of a group of three local atomic reactivity indices of atoms of the common skeleton explains about 92% of the variation of $\log(K_i)$. Figure 7, spanning about 2.1 orders of magnitude, shows that there is a good correlation of observed *versus* calculated values and that almost all points are inside the 95% confidence interval.

Results for Case 3

The common skeleton for this case is shown below (Fig. 8).

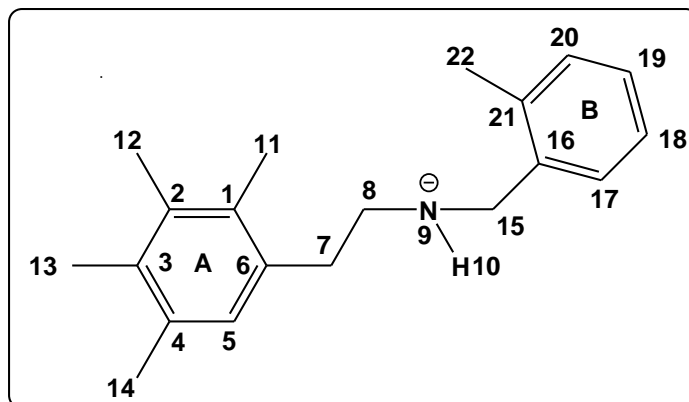


Figure 8: Common skeleton numbering for case 3

The best statistically significant equation obtained was:

$$\log(K_i) = -12.17 + 0.003S_{15}^N + 1.22\eta_9 + 52.81F_8(\text{HOMO})^* \quad (4)$$

with $n=12$, $R=0.99$, $R^2=0.97$, $\text{adj-}R^2=0.96$, $F(3,8)=99.62$ ($p<0.000001$) and a standard error of estimate of 0.14. No outliers were detected and no residuals fall outside the $\pm 2\sigma$ limits. Here, S_{15}^N is the total atomic nucleophilic superdelocalizability of atom 15, η_9 is the local atomic hardness of atom 9 and F_8 is the Fukui index of the highest occupied MO localized on atom 8. Tables 8 and 9 show the beta coefficients, the results of the t-test for significance of variable and the matrix of squared correlation coefficients for the variables of Eq. 4. There are no significant internal correlations between independent variables (Table 9). Figure 9 displays the plot of observed *vs.* calculated $\log(K_i)$.

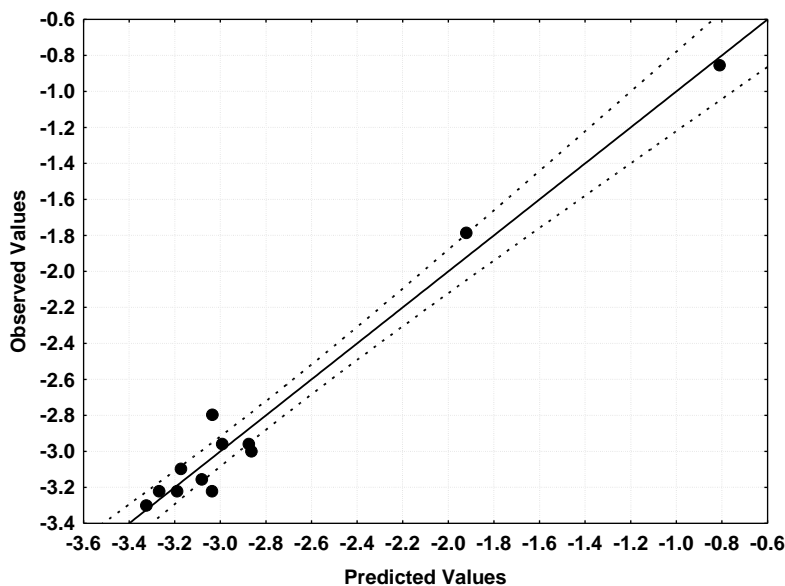


Figure 9: Plot of predicted *vs.* observed $\log(K_i)$ values (Eq. 4). Dashed lines denote the 95% confidence interval

Table 8: Beta coefficients and t-test for significance of coefficients in Eq. 4

Variable	Beta	B	t(8)	p-level
S_{15}^N	0.77	0.003	11.07	0.000004
η_9	0.30	1.22	4.90	0.001
$F_8(\text{HOMO})^*$	0.25	52.81	3.46	0.009

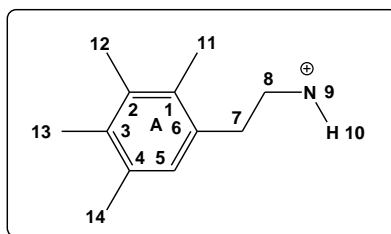
Table 9: Matrix of squared correlation coefficients for the variables in Eq. 4

	S_{15}^N	η_9	$F_8(\text{HOMO})^*$
S_{15}^N	1.00		
η_9	0.00	1.00	
$F_8(\text{HOMO})^*$	0.28	0.08	1.00

The associated statistical parameters of Eq. 4 indicate that this equation is statistically significant and that the variation of the numerical values of a group of three local atomic reactivity indices of atoms of the common skeleton explains about 96% of the variation of $\log(K_i)$. Figure 9, spanning about 2.8 orders of magnitude, shows that there is a good correlation of observed *versus* calculated values and that almost all points are inside the 95% confidence interval.

Results for Case 4

The common skeleton for this case is shown below (Fig. 10).

**Figure 10:** Common skeleton numbering for case 4

The best statistically significant equation obtained was:

$$\log(K_i) = 8.48 + 30.97S_{10}^E - 0.004\phi_{R3} - 1.62S_3^E - 2.17F_5(\text{LUMO})^* \quad (5)$$

with $n=12$, $R=0.99$, $R^2=0.97$, $\text{adj-}R^2=0.96$, $F(4,7)=59.83$ ($p<0.00002$) and a standard error of estimate of 0.22. No outliers were detected and no residuals fall outside the $\pm 2\sigma$ limits. Here, S_{10}^E is the total atomic electrophilic superdelocalizability, ϕ_{R3} is the orientational parameter of the R_3 substituent, S_3^E is the total atomic electrophilic superdelocalizability of atom 3 and $F_5(\text{LUMO})^*$ is the Fukui index of the lowest empty MO localized on atom 5. Tables 10 and 1 show the beta coefficients, the results of the t-test for significance of variable and the matrix of squared correlation coefficients for the variables of Eq. 5. There are no significant internal correlations between independent variables (Table 11). Figure 11 displays the plot of observed *vs.* calculated $\log(K_i)$.

Table 10: Beta coefficients and t-test for significance of coefficients in Eq. 5

Variable	Beta	t(7)	p-level
S_{10}^E	1.01	14.47	0.000002
ϕ_{R3}	-0.52	-7.69	0.0001
S_3^E	-0.45	-5.99	0.0005
$F_5(\text{LUMO})^*$	-0.28	-3.61	0.009

Table 11: Matrix of squared correlation coefficients for the variables in Eq. 5

	S_{10}^E	ϕ_{R3}	S_3^E	$F_5(\text{LUMO})^*$
S_{10}^E	1.00			
ϕ_{R3}	0.00	1.00		
S_3^E	0.05	0.02	1.00	
$F_5(\text{LUMO})^*$	0.02	0.05	0.20	1.00



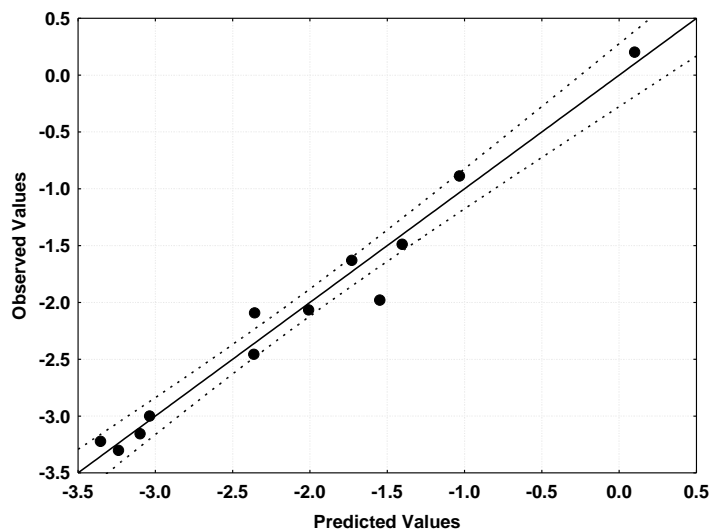


Figure 11: Plot of predicted vs. observed $\log(K_i)$ values (Eq. 5). Dashed lines denote the 95% confidence interval. The associated statistical parameters of Eq. 5 indicate that this equation is statistically significant and that the variation of the numerical values of a group of four local atomic reactivity indices of atoms of the common skeleton explains about 96% of the variation of $\log(K_i)$. Figure 11, spanning about 4 orders of magnitude, shows that there is a good correlation of observed *versus* calculated values and that almost all points are inside the 95% confidence interval.

Local molecular orbitals

Tables 12-14 show the local MO structure of atoms appearing in Eq. 1-4 (Nomenclature: Molecule (HOMO) / (HOMO-2)* (HOMO-1)* (HOMO)* - (LUMO)* (LUMO+1)* (LUMO+2)*).

Table 12: Local molecular orbitals of atoms 1-3, 5 and 6

Mol.	Atom 1	Atom 2	Atom 3	Atom 5	Atom 6
1 (66)	66 π -68 π	66 π -67 σ			
2 (57)	57 π -59 π	57 π -58 σ			
3 (53)	53 π -55 π	53 π -54 σ			
4 (57)	57 π -59 π	57 π -58 σ			
5 (98)	98 π -101 π	98 π -101 π	98 π -100 π	98 π -100 π	98 π -100 π
6 (89)	89 π -92 π				
7 (85)	85 π -88 π				
8 (89)	89 π -92 π				
9 (49)	49 π -51 π	49 π -50 σ			
10 (75)	75 π -77 π	74 π -77 π	75 π -77 π	75 π -77 π	75 π -76 σ
11(60)	60 π -61 π				
12 (61)	61 π -63 π	61 π -62 σ			
13 (81)	81 π -84 π				
14 (107)	107 π -110 π				
15 (92)	92 π -93 π				
16 (93)	93 π -96 π				
17 (65)	65 π -67 π	65 π -66 σ			
18 (69)	69 π -71 π	69 π -70 σ			
19 (69)	69 π -71 π	69 π -70 σ			
20 (57)	57 π -59 π	57 π -59 π	57 π -59 π	56 π -59 π	57 π -58 σ
21 (97)	97 π -100 π	96 π -100 π	97 π -100 π	97 π -100 π	97 π -100 π
22 (97)	97 π -100 π	96 π -100 π	97 π -100 π	97 π -100 π	97 π -100 π
23 (101)	101 π -104 π				



24 (89)	89 π -92 π				
---------	--------------------	--------------------	--------------------	--------------------	--------------------

Table 13: Local molecular orbitals of atoms 7-10

Mol.	Atom 7	Atom 8	Atom 9	Atom 10
1 (66)	63 σ - 67 σ	66 σ - 67 σ	54 σ - 68 σ	47 σ - 67 σ
2 (57)	52 σ - 58 σ	57 σ - 58 σ	45 σ - 59 σ	38 σ - 58 σ
3 (53)	52 σ - 54 σ	53 σ - 54 σ	41 σ - 55 σ	38 σ - 54 σ
4 (57)	56 σ - 58 σ	57 σ - 58 σ	43 σ - 59 σ	40 σ - 58 σ
5 (98)	93 σ - 99 σ	98 σ -100 σ	94 σ - 99 σ	75 σ - 99 σ
6 (89)	81 σ - 90 σ	89 σ - 91 σ	85 σ - 90 σ	67 σ - 91 σ
7 (85)	84 σ - 86 σ	84 σ - 88 σ	82 σ - 86 σ	62 σ - 87 σ
8 (89)	88 σ - 90 σ	89 σ - 92 σ	86 σ - 90 σ	64 σ - 91 σ
9 (49)	48 σ - 50 σ	48 σ - 50 σ	39 σ - 51 σ	36 σ - 50 σ
10 (75)	72 σ - 76 σ	75 σ - 76 σ	63 σ - 77 σ	60 σ - 76 σ
11(60)	54 σ - 61 σ	56 σ - 61 σ	48 σ - 61 σ	45 σ - 62 σ
12 (61)	60 σ - 62 σ	61 σ - 62 σ	46 σ - 63 σ	42 σ - 62 σ
13 (81)	80 σ - 84 σ	80 σ - 82 σ	78 σ - 82 σ	62 σ - 83 σ
14 (107)	103 σ -110 σ	107 σ -108 σ	104 σ -108 σ	86 σ -109 σ
15 (92)	84 σ - 93 σ	89 σ - 93 σ	86 σ - 94 σ	71 σ - 95 σ
16 (93)	92 σ - 96 σ	93 σ - 94 σ	90 σ - 94 σ	68 σ - 95 σ
17 (65)	60 σ - 66 σ	63 σ - 66 σ	49 σ - 67 σ	46 σ - 66 σ
18 (69)	66 σ - 70 σ	66 σ - 70 σ	52 σ - 71 σ	48 σ - 70 σ
19 (69)	67 σ - 70 σ	69 σ - 70 σ	52 σ - 71 σ	48 σ - 70 σ
20 (57)	57 σ - 58 σ	57 σ - 58 σ	46 σ - 59 σ	38 σ - 58 σ
21 (97)	90 σ -100 σ	95 σ - 98 σ	93 σ - 98 σ	72 σ - 99 σ
22 (97)	90 σ -100 σ	95 σ - 98 σ	93 σ - 98 σ	72 σ - 99 σ
23 (101)	98 σ -104 σ	101 σ -102 σ	97 σ -102 σ	75 σ -103 σ
24 (89)	84 σ - 90 σ	89 σ - 90 σ	85 σ - 90 σ	62 σ - 90 σ

Table 14: Local molecular orbitals of atoms 13 and 14

Mol.	Atom 13	Atom 15
1 (66)	66 π - 68 π	----
2 (57)	57 π - 59 π	----
3 (53)	53 σ - 56 σ	----
4 (57)	56 σ - 60 σ	----
5 (98)	98 π -101 π	94 σ - 99 σ
6 (89)	89 π - 92 π	85 σ - 90 σ
7 (85)	85 σ - 90 σ	82 σ - 86 σ
8 (89)	88 σ - 94 σ	86 σ - 90 σ
9 (49)	46 σ - 56 σ	----
10 (75)	70 σ - 78 σ	----
11(60)	59 π - 61 π	----
12 (61)	60 σ - 64 σ	----
13 (81)	76 σ - 92 σ	78 σ - 82 σ
14 (107)	107 π -110 π	102 σ -108 σ
15 (92)	90 π - 93 π	86 σ - 94 σ
16 (93)	92 σ - 98 π	90 σ - 94 σ
17 (65)	65 π - 67 π	----
18 (69)	69 π - 71 π	----
19 (69)	69 π - 71 π	----
20 (57)	57 π - 59 π	----
21 (97)	97 π -100 π	93 σ - 98 σ
22 (97)	97 π -100 π	93 σ - 98 σ
23 (101)	101 π -104 π	97 σ -102 σ
24 (89)	89 π - 92 π	85 σ - 90 σ



Discussion

Molecular orbitals and local molecular orbitals

Here we present some pictographic examples to clarify the concepts of ‘molecular orbital’ and ‘local molecular orbital’. In our model we have stated that we may say that a certain MO is localized on atom i if the corresponding Fukui index is greater than $0.01e$. Notice that this value of the Fukui index was selected for these kinds of biologically active molecules and may vary for the case of other different chemical structures, such as nanostructures. Figure 12 shows the HOMO of molecule 1.

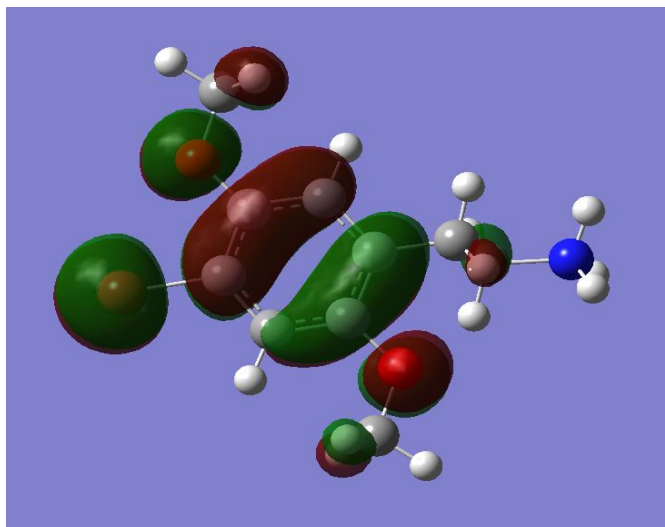


Figure 12: HOMO of molecule 1

We can see that this MO has π character on the atoms of the phenyl ring and on the oxygen and bromine atoms bonded to it. On the carbon atom of the side chain this MO has a σ character. In Tables 12-14 we can see that this particular MO corresponds to the local highest occupied MO, called HOMO*, of atoms 1-3, 5-6 and 8 (Fig. 2). Figure 13 shows the (HOMO-3) (i.e., the fourth highest occupied MO) of molecule 1.

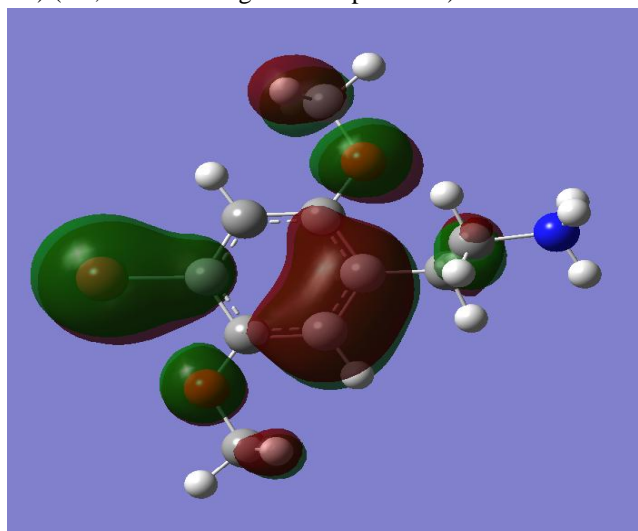


Figure 13: (HOMO-3) of molecule 1

We can see here that this MO has π and σ regions. Table 13 shows that this MO corresponds to the local HOMO* of atom 13 (Fig. 6). Fig. 14 shows the twelfth highest occupied MO of molecule 1.

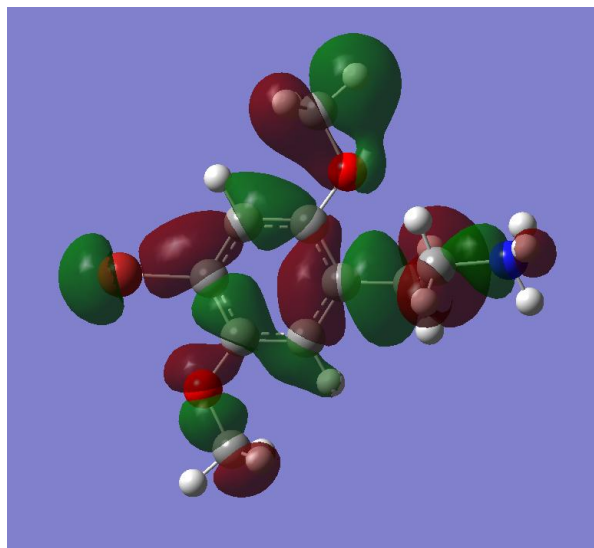


Figure 14: (HOMO-12) of molecule 1

This MO has a σ character and corresponds to the local HOMO* of atom 9, a substituted nitrogen atom (Fig. 2). The discussion will be presented as follows. In each case we will analyze only the most statistically significant variables. For these variables an atom (drug)- atom (receptor) interaction will be suggested. For the discussion of the meaning of the reactivity indices in each equation, we shall employ the method recently published ¹⁶.

Discussion of case 1A

The beta values (Table 2) show that the most significant variables in Eq. 1 are s_9 , S_9^N and $F_8(\text{HOMO})^*$. As $F_6(\text{HOMO})^*$ and η_7 are less significant they will not be discussed. A high receptor binding affinity is associated with high numerical values of s_9 (that is always a positive number), with small numerical values of S_9^N (if we consider it to be a positive number, see XX) and $F_8(\text{HOMO})^*$ (that is always a positive number). Atom 9 is the nitrogen atom of the ethylamine side chain (Fig. 2). Table 13 shows that all local MOs have a σ nature and that the local HOMO is an inner MO of the respective molecule. The same Table shows that $(\text{LUMO})_9^*$ coincides with the molecule's LUMO or $(\text{LUMO}+1)$. Higher values of this reactivity index are associated with higher receptor binding. Higher values correspond to higher values of the local softness implying lower values of the local atomic hardness (LAH). The inspection of the specific local molecular orbital structure of this atom indicates that lower values of the LAH are obtained when $(\text{HOMO})_9^*$ coincides with the molecular HOMO. Then, a greater activity seems to be associated with a better electron-donor capacity of atom 9. This suggestion is indirectly supported by the fact that small values for S_9^N are required for high activity. These smaller values are obtained by raising the LUMO_9^* energy, making this MO less reactive. Note that in the case of 2,5-dimethoxyphenethylamines HOMO_9^* corresponds to 'inner' occupied molecular MOs while in the case of their N-2-methoxybenzyl-substituted analogs HOMO_9^* corresponds to 'outer' molecular MOs close to the HOMO. One possibility is that atom 9 participates in weak $\sigma_{\text{occ}}-\sigma_{\text{empty}}$ interactions. An alternative possibility is that this atom participates in a hydrogen bond of the N-H...X kind. Atom 8 is a saturated carbon in the ethylamine chain (Fig. 2). Table 13 shows that all local MOs have a σ nature. The local HOMO is of sigma nature and coincides with the molecule's HOMO. Very small values of $F_8(\text{HOMO})^*$ are associated with high binding affinity, signifying that this atom is not acting as an electron donor. This can be an indication that atom 8 is acting through its LUMO_8^N in $\sigma_{\text{empty}}-\sigma_{\text{occ}}$ interactions. All the suggestions are displayed in the partial 2D pharmacophore of Fig. 15.



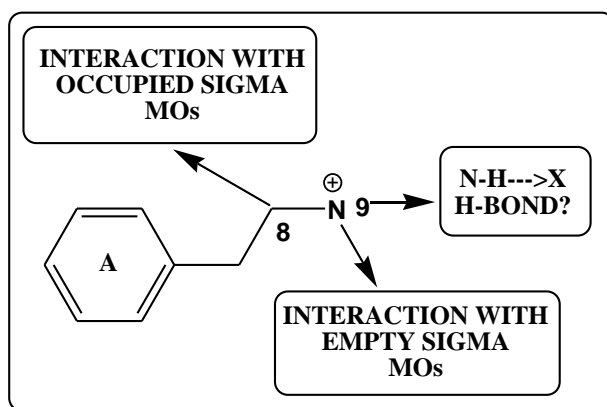


Figure 15: Partial 2D pharmacophore for Eq. 1

Discussion of case 1B

The beta values (Table 4) show that the most significant variables in Eq. 2 are ϕ_{benz} , $F_8(\text{HOMO})^*$ and $F_3(\text{HOMO})^*$. A high receptor binding affinity is associated with high numerical values of ϕ_{benz} and with low numerical values for $F_8(\text{HOMO})^*$ and $F_3(\text{HOMO})^*$. The orientational parameter (OP) of the benzyl moiety. A high binding affinity is associated with a high numerical value for this OP. The highest possible value corresponds to the most extended conformer of the benzyl group. Figure 16 shows, as an example, the ten lowest energy conformers of molecule 6 calculated with MarvinView (version 17.28.0, 2017, ChemAxon, <http://www.chemaxon.com>) with the Dreiding force field, a diversity of 0.5 kcal/mol, very strict optimization limit and a time of 900s. The conformers were superimposed with the 2,5-dimethoxy-4-Cl-phenyl moiety as the common element.

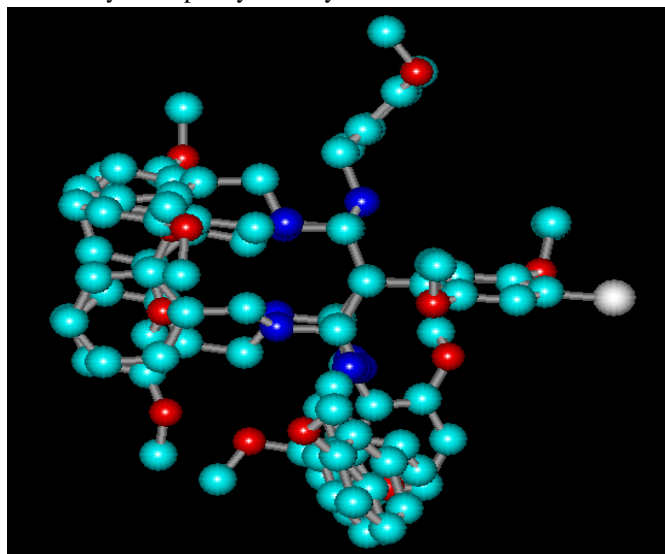


Figure 16: Superimposition of ten lowest-energy conformers of molecule 6

We can see that at the left side of the figure there are five extended conformers. These conformers will be more stable in a polar environment, such as the cell milieu plus some regions or the entire binding site. At the center of the figure we can see five half-closed conformers that will be stable in a hydrophobic environment. Atom 8 was discussed in case 1A and the conclusions are the same. Atom 3 is a carbon in the phenyl ring where the 5-substituent is attached (Fig. 4). Table 12 shows that all local frontier MOs have a π nature and that the local HOMO_3^* coincides with the molecular HOMO in all cases. A high binding affinity is associated with low values for $F_3(\text{HOMO})^*$ which means a MO with a low electron population. On this basis we suggest that atom 3 is interacting with an electron-rich center. All the suggestions are displayed in the partial 2D pharmacophore of Fig. 17.

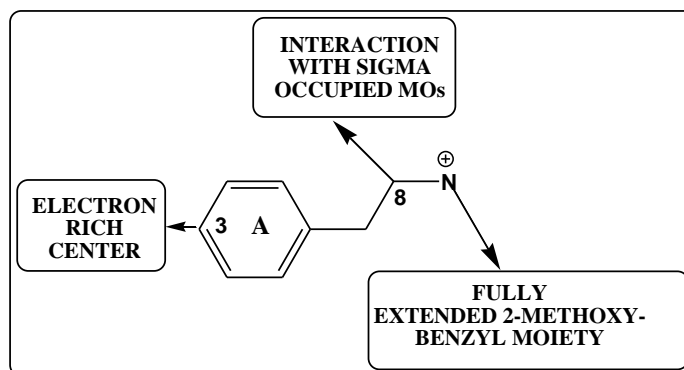


Figure 17: Partial 2D pharmacophore for Eq. 2

Discussion of Case 2

The beta values (Table 6) show that the most significant variables in Eq. 3 are μ_9 and $S_{13}^N(\text{LUMO})^*$. Eq. 3 shows that a high binding affinity is associated with small (negative) values of μ_9 and small (positive) values for $S_{13}^N(\text{LUMO})^*$. Atom 9 is the nitrogen atom of the side chain of phenylalkylamines (Fig. 6). Table 13 shows that all local MOs have a σ nature, that local LUMO_9^* is close to the molecule's LUMO or coincides with it, that in phenylalkylamines the local HOMO_9^* corresponds to an inner occupied molecular MO and that in N-2-methoxybenzyl-substituted analogs HOMO_9^* corresponds to molecular MOs close to the HOMO. μ_9 is a negative number and small negative values for this index can be obtained directly from the definition of this index. In the case in which the local HOMO_9^* coincides with the molecule's HOMO we may increase the energy of the LUMO_9^* making it less reactive. This method can be applied to N-2-methoxybenzyl-substituted analogs. If HOMO_9^* corresponds to an inner occupied molecular MO we may use substitution(s) to localize the molecular HOMO on atom 9. This is the case of phenylalkylamines. In this case we are increasing the reactivity of HOMO_9^* . On the basis of this reasoning we suggest that atom 9 is interacting with sigma empty MOs. A different possibility is that the N atom participates as an electron donor in a hydrogen bond of the N-H \rightarrow X kind. Atom 13 is the first atom of the substituent attached to position 3 (see Fig. 6 and Table 1). Small (positive) values of $S_{13}^N(\text{LUMO})^*$ are associated with high affinity. Table 14 shows that LUMO_{13}^* has π or σ nature following the molecule. The formal definition of the orbital superdelocalizability allows two ways of obtaining the desired values. The first one consists in diminishing the electron population of this MO on atom 13 (i.e., diminishing the value of the corresponding Fukui index). The second one is simply by using substitutions to change the actual LUMO_{13}^* by a higher empty molecular MO (i.e., by removing the localization of the actual LUMO_{13}^* on atom 9). Both ways lead to empty MOs with diminished reactivity. Therefore, it is suggested that atom 13 is interacting with the site through its occupied MOs, especially HOMO_{13}^* . Now, considering that this MO has π or σ nature following the molecule, it is possible to think in an electrostatic interaction with one site or in a MO-MO interaction with two sites, one with π empty MOs and the other with σ empty MOs. All the suggestions are displayed in the partial 2D pharmacophore of Fig. 18.

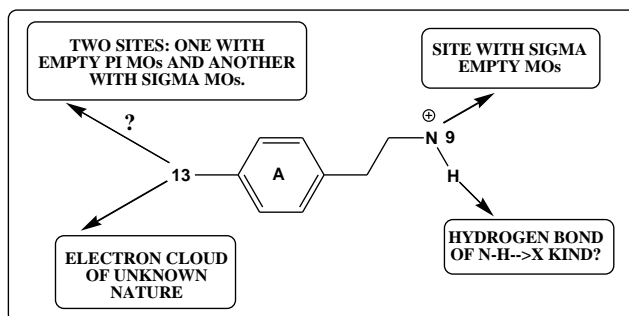


Figure 18: Partial 2D pharmacophore for Eq. 3



Discussion of Case 3

The beta values (Table 8) show that the most significant variable in Eq. 4 is S_{15}^N . Eq. 4 specifies that a high binding affinity is associated with small (positive) values for S_{15}^N . Atom 15 is a sp^3 carbon in the chain connecting rings A and B, bonded to ring B (Fig. 8). All MOs have a σ nature. Table 14 shows that the local LUMO, $(LUMO)_{15}^*$, coincides with the molecule's LUMO in all cases. A small positive value for S_{15}^N is obtained by shifting upwards the energy of $(LUMO)_{15}^*$ and upper empty MOs, making these MOs less reactive. Therefore we suggest that atom 15 is interacting with a site with empty MOs through its occupied MOs. All the suggestions are displayed in the partial 2D pharmacophore of Fig. 19.

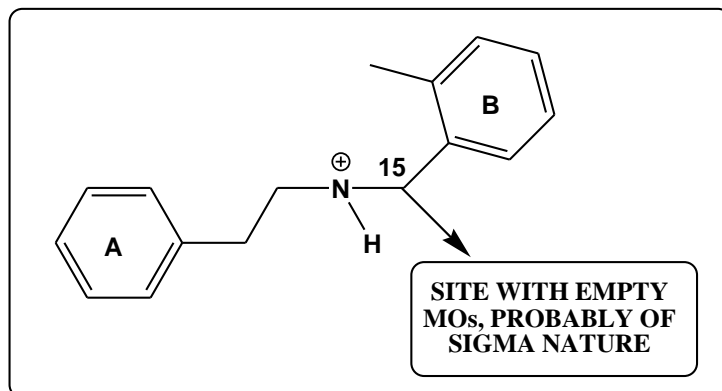


Figure 19: Partial 2D pharmacophore for Eq. 4

Discussion of Case 4

The beta values (Table 10) show that the most significant variables in Eq. 5 are S_{10}^E , φ_{R3} and S_3^E . Eq. 5 shows that a high binding affinity is associated with high (negative) values of S_{10}^E , large positive values for φ_{R3} and small (negative) values for S_3^E . φ_{R3} is the orientational parameter of the substituent attached to atom 3 (Fig. 10). Large values for φ_{R3} indicate that larger and fully extended substituents should be appropriate: OEt instead of OMe, Et instead of Me, etc. Nevertheless when varying the substituents, their chemical nature should be similar: for example, you cannot change a bromine atom by fluorine one or a Me group by a COOH one. Atom 10 is a hydrogen atom attached to N9 (Fig. 10). A high affinity is associated with large values for S_3^E . This reactivity index is indicative of the electron-donating capacity. On the other hand, $(HOMO)_{10}^*$ corresponds to a molecule's inner occupied MO (Table XX). These facts are contradictory and the only way to conciliate them is by suggesting that this atom is serving as a bridge for a N-H...X hydrogen bond. Atom 3 is a carbon atom in ring A (Fig. 10). High affinity is associated with low (negative) numerical values of S3E. Remember that $(HOMO)_3^*$ is the dominant term in the definition of the atomic electrophilic superdelocalizability. These values can be obtained by making more negative the $(HOMO)_3^*$ energy, by making smaller the population of $(HOMO)_3^*$ or by both procedures. This lowers the electron-donor capacity of atom 3. Therefore, this atom seems to interact with an electron-rich center. All the suggestions are displayed in the partial 2D pharmacophore of Fig. 20.

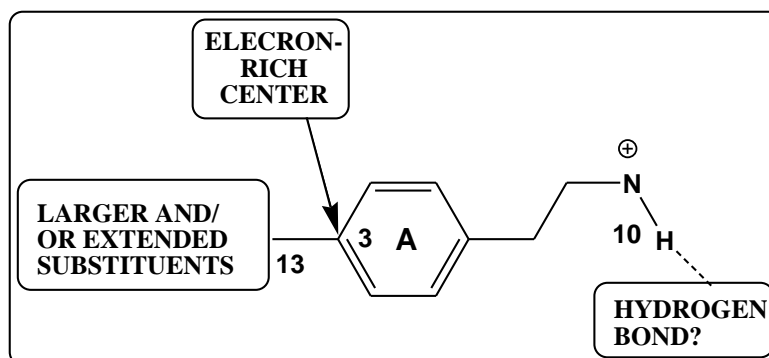


Figure 20: Partial 2D pharmacophore for Eq. 5

Integration of the Results

The integration of the results is carried out by building a larger partial 2D pharmacophore including all the pharmacophores suggested for each case. It is shown in Fig. 21.

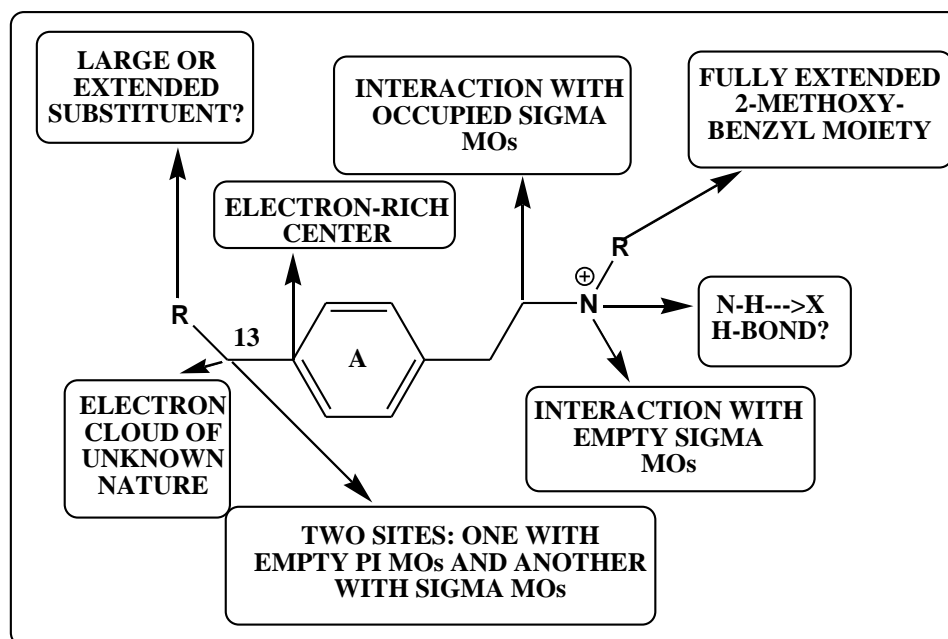


Figure 21: Final 2D partial pharmacophore for the molecule-5-HT_{2A} serotonin receptor interactions

In summary, we have obtained a detailed partial pharmacophore for the interaction of 24 molecules with the with the 5-HT_{2A} serotonin receptors. This construct, together with the ones obtained in previous studies should help to have a better idea of the molecule-receptor interaction and to design new molecular structures with enhanced activity.

References

- Gómez-Jeria, J. S. Approximate Molecular Electrostatic Potentials of Protonated Mescaline Analogues. *Acta sud Americana de Química* 1984, 4, 1-9.
- Gómez-Jeria, J. S.; Morales-Lagos, D. The mode of binding of phenylalkylamines to the Serotonergic Receptor. In *QSAR in design of Bioactive Drugs*, Kuchar, M., Ed. Prous, J.R.: Barcelona, Spain, 1984; pp 145-173.
- Gómez-Jeria, J. S.; Morales-Lagos, D. R. Quantum chemical approach to the relationship between molecular structure and serotonin receptor binding affinity. *Journal of Pharmaceutical Sciences* 1984, 73, 1725-1728.
- Gómez-Jeria, J. S.; Morales-Lagos, D.; Rodriguez-Gatica, J. I.; Saavedra-Aguilar, J. C. Quantum-chemical study of the relation between electronic structure and pA2 in a series of 5-substituted tryptamines. *International Journal of Quantum Chemistry* 1985, 28, 421-428.
- Gómez-Jeria, J. S.; Morales-Lagos, D.; Cassels, B. K.; Saavedra-Aguilar, J. C. Electronic structure and serotonin receptor binding affinity of 7-substituted tryptamines. *Quantitative Structure-Activity Relationships* 1986, 5, 153-157.
- Gómez-Jeria, J. S.; Cassels, B. K.; Saavedra-Aguilar, J. C. A quantum-chemical and experimental study of the hallucinogen (\pm)-1-(2,5-dimethoxy-4-nitrophenyl)-2-aminopropane (DON). *European Journal of Medicinal Chemistry* 1987, 22, 433-437.
- Richter, P.; Morales, A.; Gomez-Jeria, J. S.; Morales-Lagos, D. Electrochemical study of the hallucinogen (\pm)-1-(2,5-dimethoxy-4-nitrophenyl)-2-aminopropane. *Analyst* 1988, 113, 859-863.



8. Gómez-Jeria, J. S.; Robles-Navarro, A. A Density Functional Theory and Docking study of the Relationships between Electronic Structure and 5-HT_{2B} Receptor Binding Affinity in N-Benzyl Phenethylamines. *Der Pharma Chemica* 2015, 7, 243-269.
9. Gómez-Jeria, J. S.; Robles-Navarro, A. A Note on the Docking of some Hallucinogens to the 5-HT_{2A} Receptor. *Journal of Computational Methods in Molecular Design* 2015, 5, 45-57.
10. Gómez-Jeria, J. S.; Robles-Navarro, A. DFT and Docking Studies of the Relationships between Electronic Structure and 5-HT_{2A} Receptor Binding Affinity in N-Benzylphenethylamines. *Research Journal of Pharmaceutical, Biological and Chemical Sciences* 2015, 6, 1811-1841.
11. Gómez-Jeria, J. S.; Robles-Navarro, A. A Quantum Chemical Study of the Relationships between Electronic Structure and cloned rat 5-HT_{2C} Receptor Binding Affinity in N-Benzylphenethylamines. *Research Journal of Pharmaceutical, Biological and Chemical Sciences* 2015, 6, 1358-1373.
12. Gómez-Jeria, J. S.; Abuter-Márquez, J. A Theoretical Study of the Relationships between Electronic Structure and 5-HT_{1A} and 5-HT_{2A} Receptor Binding Affinity of a group of ligands containing an isonicotinic nucleus. *Chemistry Research Journal* 2017, 2, 198-213.
13. Gómez-Jeria, J. S.; Becerra-Ruiz, M. B. Electronic structure and rat fundus serotonin receptor binding affinity of phenethylamines and indolealkylamines. *International Journal of Advances in Pharmacy, Biology and Chemistry* 2017, 6, 72-86.
14. Gómez-Jeria, J. S.; Moreno-Rojas, C. Dissecting the drug-receptor interaction with the Klopman-Peradejordi-Gómez (KPG) method. I. The interaction of 2,5-dimethoxyphenethylamines and their N-2-methoxybenzyl-substituted analogs with 5-HT_{1A} serotonin receptors. *Chemistry Research Journal* 2017, 2, 27-41.
15. Rickli, A.; Luethi, D.; Reinisch, J.; Buchy, D.; Hoener, M. C.; Liechti, M. E. Receptor interaction profiles of novel N-2-methoxybenzyl (NBOMe) derivatives of 2,5-dimethoxy-substituted phenethylamines (2C drugs). *Neuropharmacology* 2015, 99, 546-553.
16. Gómez-Jeria, J. S.; Kpotin, G. Some Remarks on The Interpretation of The Local Atomic Reactivity Indices Within the Klopman-Peradejordi-Gómez (KPG) Method. I. Theoretical Analysis. *Research Journal of Pharmaceutical, Biological and Chemical Sciences* 2018, 9, 550-561.
17. Gómez-Jeria, J. S. 45 Years of the KPG Method: A Tribute to Federico Peradejordi. *Journal of Computational Methods in Molecular Design* 2017, 7, 17-37.
18. Gómez-Jeria, J. S. A New Set of Local Reactivity Indices within the Hartree-Fock-Roothaan and Density Functional Theory Frameworks. *Canadian Chemical Transactions* 2013, 1, 25-55.
19. Gómez-Jeria, J. S. *Elements of Molecular Electronic Pharmacology (in Spanish)*. 1st ed.; Ediciones Sokar: Santiago de Chile, 2013; p 104.
20. Gómez-Jeria, J. S.; Ojeda-Vergara, M. Parametrization of the orientational effects in the drug-receptor interaction. *Journal of the Chilean Chemical Society* 2003, 48, 119-124.
21. Gómez-Jeria, J. S. Modeling the Drug-Receptor Interaction in Quantum Pharmacology. In *Molecules in Physics, Chemistry, and Biology*, Maruani, J., Ed. Springer Netherlands: 1989; Vol. 4, pp 215-231.
22. Gómez-Jeria, J. S. On some problems in quantum pharmacology I. The partition functions. *International Journal of Quantum Chemistry* 1983, 23, 1969-1972.
23. Gómez-Jeria, J. S. La Pharmacologie Quantique. *Bollettino Chimico Farmaceutico* 1982, 121, 619-625.
24. Note. The results presented here are obtained from what is now a routinary procedure. For this reason, we built a general model for the paper's structure. This model contains *standard* phrases for the presentation of the methods, calculations and results because they do not need to be rewritten repeatedly. In 2018.
25. Frisch, M. J.; Trucks, G. W.; Schlegel, H. B.; Scuseria, G. E.; Robb, M. A.; Cheeseman, J. R.; Montgomery, J., J.A.; Vreven, T.; Kudin, K. N.; Burant, J. C.; Millam, J. M.; Iyengar, S. S.; Tomasi, J.; Barone, V.; Mennucci, B.; Cossi, M.; Scalmani, G.; Rega, N. *G03 Rev. E.01*, Gaussian: Pittsburgh, PA, USA, 2007.



26. Gómez-Jeria, J. S. *D-Cent-QSAR: A program to generate Local Atomic Reactivity Indices from Gaussian 03 log files*. v. 1.0, v. 1.0; Santiago, Chile, 2014.
27. Gómez-Jeria, J. S. An empirical way to correct some drawbacks of Mulliken Population Analysis (Erratum in: J. Chil. Chem. Soc., 55, 4, IX, 2010). *Journal of the Chilean Chemical Society* 2009, 54, 482-485.
28. Gómez-Jeria, J. S. Tables of proposed values for the Orientational Parameter of the Substituent. II. *Research Journal of Pharmaceutical, Biological and Chemical Sciences* 2016, 7, 2258-2260.
29. Gómez-Jeria, J. S. Tables of proposed values for the Orientational Parameter of the Substituent. I. Monoatomic, Diatomic, Triatomic, n-CnH_{2n+1}, O-n-CnH_{2n+1}, NRR', and Cycloalkanes (with a single ring) substituents. *Research Journal of Pharmaceutical, Biological and Chemical Sciences* 2016, 7, 288-294.
30. Gómez-Jeria, J. S. *STERIC: A program for calculating the Orientational Parameters of the substituents* 2.0; Santiago, Chile, 2015.
31. Statsoft. *Statistica* v. 8.0, 2300 East 14 th St. Tulsa, OK 74104, USA, 1984-2007.

